Journal of Catalysis 261 (2009) 201–207

Contents lists available at ScienceDirect

Journal of Catalysis

www.elsevier.com/locate/jcat

Influence of Pt location on $BaCO_3$ or Al_2O_3 during NO_x storage reduction

Robert Büchel [a,b], Reto Strobel [a], Frank Krumeich [b], Alfons Baiker [b], Sotiris E. Pratsinis [a,*]

[a] Particle Technology Laboratory, Department of Mechanical and Process Engineering, ETH Zurich, Sonneggstrasse 3, CH-8092 Zurich, Switzerland
[b] Department of Chemistry and Applied Biosciences, ETH Zurich, Hönggerberg, HCI, CH-8093 Zurich, Switzerland

ARTICLE INFO

Article history:
Received 17 September 2008
Revised 14 November 2008
Accepted 21 November 2008
Available online 11 December 2008

Keywords:
NO_x storage–reduction
$Pt/Ba/Al_2O_3$
Flame spray pyrolysis
Pt–Ba proximity
Remote control
Lean NO_x trap

ABSTRACT

Catalysts for NO_x storage–reduction (NSR) were made selectively with Pt on either the Al- or the Ba-components without altering significantly the Al_2O_3 or $BaCO_3$ crystal sizes, Al/Ba weight ratio, specific surface area, porosity, and Pt dispersion using a two-nozzle flame spray pyrolysis (FSP) unit. The NO_x storage performance at 300 °C was best for Pt located near Al_2O_3 as it facilitates the oxidation of NO to NO_2 during the fuel lean period but the reduction rate during the subsequent short fuel rich period was much slower resulting in incomplete regeneration. This contributed to a gradual decrease of the NO_x conversion at increasing cycling. In contrast, Pt on $BaCO_3$ resulted in an initially lower NO_x storage rate but during ten storage–reduction cycles a stable NO_x conversion of about 50% was reached. When using NO_2 instead of NO or higher NO_x oxidation-reduction temperatures (e.g. 350 °C) the Pt location did not affect the NSR performance of the $Pt/Ba/Al_2O_3$ catalysts.

© 2008 Elsevier Inc. All rights reserved.

1. Introduction

Anthropogenic NO_x is formed typically during fuel combustion contributing to smog formation and acid rain [1,2]. New catalysts are needed to meet stricter emission limits, especially to remove NO_x under oxygen rich conditions of lean fuel and direct injection engines. Among these catalysts, the ones for NO_x storage–reduction (NSR) can trap exhaust NO_x on an alkali- or alkaline earth metal (typically Ba or K) in the form of metal-nitrates [3] without requiring an additional reducing agent, as NH_3 or urea in selective catalytic reduction (SCR). During a subsequent fuel rich period the stored metal-nitrates are reduced to harmless N_2 over a noble metal (typically Pt or Pd) [4]. The storage and the noble metal are supported on a thermally stable carrier material, usually Al_2O_3 or CeO_2 [5]. Pt-free BaO/Al_2O_3 mainly stored NO_2, whereby releasing one NO for three NO_2 stored [6]. In the presence of Pt, NO is oxidized to NO_2 resulting in higher storage capacity and faster NO_x uptake [7], involving NO_2 spillover from the Pt to the Ba sites as proposed from simulations [8] and experimental investigations [9]. Already in 1995 the proximity of Pt to the storage component of NSR catalysts was proposed to strongly influence the performance [10] and was recently investigated by comparing ternary $Pt/Ba/Al_2O_3$ catalysts with binary mixtures of Pt/Al_2O_3 and Ba/Al_2O_3 [11]. For Pt in close contact with Ba a 5-times higher isotopic exchange rate between ^{15}NO was measured, indicative of NO_x forward and reverse spillover from Pt to Ba [11].

In contrast to storage, the reduction (regeneration) is less understood mainly due to parallel occurring phenomena such as the desorption of gaseous NO_x at high temperature [12] and the reaction of the stored nitrate with CO_2 [13,14]. Nova et al. [15] showed that the reduction of nitrates occurs by Pt-catalyzed surface reactions involving (reverse) spillover processes and concluded that a close proximity of Ba and Pt would be necessary to increase the Ba-nitrate decomposition. Physical (mechanical) mixtures of Pt/Al_2O_3 and $BaCO_3$, Al_2O_3 and $Pt/BaCO_3$ have been used to investigate the influence of the NO_x spillover distance [11,15,16]. The multiple impregnation steps employed in these studies, however, made difficult to maintain constant material characteristics for different catalyst compositions.

Here, we investigated the importance of Pt being located close to Ba or to Al on NSR catalyst performance. The catalysts were prepared by a two-nozzle flame spray pyrolysis unit as already applied for NSR catalysts [17] with high storage capacity [18]. By this procedure, Pt can be deposited preferentially on Al_2O_3 and/or $BaCO_3$ without altering their structural properties.

2. Experimental

2.1. Apparatus and preparation

With an internozzle distance, d, of 6 cm and an angle, φ, of 160° between the two nozzles (Fig. 1), the mixing distance (m) was calculated to be 34 cm above the nozzles ($m = d\tan(\varphi/2)$) assuring complete particle formation (Pt, $BaCO_3$ and Al_2O_3) at this point [19]. The individual spray nozzles were described previously

* Corresponding author.
E-mail address: pratsinis@ptl.mavt.ethz.ch (S.E. Pratsinis).

0021-9517/$ – see front matter © 2008 Elsevier Inc. All rights reserved.
doi:10.1016/j.jcat.2008.11.016

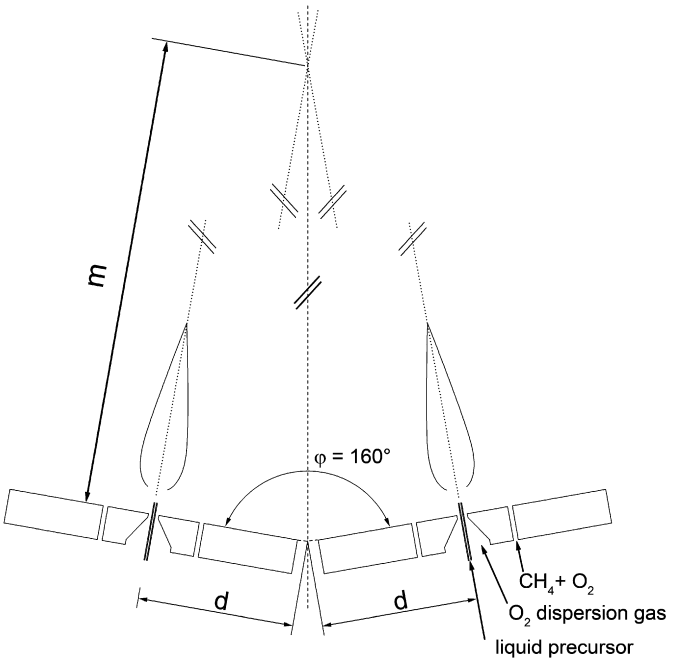

Fig. 1. Schematic of the 2-nozzle FSP unit where Al- and Ba-precursor solutions are sprayed separately. The Pt precursor is added to the Al- or Ba-precursor solutions resulting in preferential deposition of Pt-clusters on each component of the product catalyst particles. The mixing distance, m, is the distance from the burner to the crossing point of the two flame axes.

in detail [20]. The Al-precursor solution consisted of aluminum-tri-*sec*-butoxide (Fluka, 95%) dissolved in a 2:1 vol% mixture of diethylene glycol monobutyl ether (Fluka, 98%) and acetic anhydride (Riedel-de Haën, 99%). The aluminum concentration was kept constant at 0.5 mol/L. The Ba-precursor, barium 2-ethylhexanoate (Aldrich, 98%) was dissolved in 1:1 vol% toluene (Riedel-de Haën, 99%) and 2-ethylhexanoic acid (Riedel-de Haën, 95%) for a Ba concentration of 0.06 mol/L. The Pt-precursor platinum(II) acetylacetonate (STREM, 98%) was added either to the Ba or Al precursor solutions, while for an equal distribution of Pt on Al_2O_3 and $BaCO_3$ half of the platinum(II) acetylacetonate was added to each precursor solution.

For the nomenclature of all $Pt/Ba/Al_2O_3$ catalysts, the Pt is written next to the element with which it was fed to the FSP unit and precipitated on: therefore a catalyst with Pt deposited on Al_2O_3 is referred as PtAl–Ba, with Pt on $BaCO_3$ as Al–BaPt, and with Pt both on Al_2O_3 and $BaCO_3$ as PtAl–BaPt. The Ba precursor was fed at 3 mL/min through the first nozzle and the Al-precursor was fed at 5 mL/min through the second nozzle. The concentration of the metals in the precursors was chosen to result in a nominal $Pt:Ba:Al_2O_3$ weight ratio of 1:20:100. Each solution was dispersed with 5 L/min oxygen (PanGas, 99.95%) and ignited by a supporting premixed methane/oxygen flame with 3 L/min total gas flow rate and a CH_4/O_2 molar ratio of 0.5. The product powders were collected on a glass fiber filter (Whatman GF6, 25.7 cm in diameter) with the aid of a vacuum pump (Busch, Seco SV 1040C).

2.2. Materials characterization

The specific surface area (SSA) of the as-prepared powders was determined by a 5-point nitrogen adsorption isotherm at 77 K using the BET method, and a full adsorption isotherm of the as-prepared powder was measured (Micrometrics Tristar). X-ray diffraction (XRD) patterns were recorded (Bruker D8 Advance, 40 kV, 40 mA, $\lambda = 1.54$ nm) at a scan speed of 0.5°/min at $10° < 2\theta < 70°$. The effective chemical composition of pelleted powder was determined by laser-ablation inductively coupled plasma mass spectrometry (LA-ICP-MS) [21]. The Pt dispersion was measured by CO-pulse chemisorption at 40 °C on a Micromeritics Autochem II 2920. Samples were pretreated by heating in 10% O_2/He up to 500 °C (10 °C min^{-1}) and maintained for 30 min at 500 °C, then cooled in He to 350 °C where they were reduced in 5% H_2/Ar for 30 min. Subsequently, the samples were kept for another 30 min at 350 °C under flowing He before cooling to 40 °C. Pulses of 0.35 mL 10% CO/He were injected in 10% H_2/Ar and the CO concentration in the off gas was recorded using a mass spectrometer (Pfeiffer Vacuum, ThermoStar) [18].

For scanning transmission electron microscopy (STEM), the catalyst material was dispersed in ethanol and deposited onto a perforated carbon foil supported on a copper grid (Okenshoji Co. Ltd.). The STEM images were obtained with a high-angle annular dark-field (HAADF) detector attached to a Tecnai 30F microscope (FEI; field emission cathode, operated at 300 kV), showing the metal particles with bright contrast (Z contrast). For qualitative analysis, the electron beam was set to selected areas in the STEM images and the signal was measured by energy dispersive X-ray spectroscopy (EDXS; detector: EDAX).

The NO_x storage–reduction (NSR) measurements were performed with 20 mg catalyst in a fixed-bed reactor (with an inner diameter of 4 mm). The reactor was connected to a valve allowing rapid switching between oxidizing and reducing conditions [22]. The NO and NO_2 concentrations in the effluent gas were monitored using a chemiluminescence detector (ECO Physics, CLD 822S). The NO_x conversion for a full cycle (one storage and one reduction) was derived from the corresponding NO_x outlet concentration according to:

$$NO_x \text{ conversion} = \frac{NO_{x,in} - NO_{x,out}}{NO_{x,in}} \times 100\%. \quad (1)$$

The presence of N_2O was neglected here as at 300–350 °C its formation is very low [23]. The dynamic NSR behavior of as-prepared powders was measured at 300 and 350 °C by switching 10 times between oxidizing (3 min in 667 ppm NO and 3.3% O_2 in He) and reducing atmospheres (1 min in 667 ppm NO, 1333 ppm C_3H_6 in He). The total gas flow rate for all experiments was 60 mL/min corresponding to a space velocity of 72,000 h^{-1}. Complete storage and reduction tests were performed at 300 °C. The catalysts were heated to this temperature and reduced for 30 min (C_3H_6 2000 ppm, He). Then storage was recorded for 180 min with 667 ppm inlet NO or NO_2 (in He containing 3.3 vol% O_2).

3. Results and discussion

3.1. Structural properties

Preferential Pt deposition on alumina and the Ba component was confirmed by STEM combined with EDX analysis of the indicated area as shown in Fig. 2 for PtAl–Ba (A) and Al–BaPt (B) catalysts. Clusters of Pt appear as bright, spherical dots. The gray particles are assigned to Al_2O_3 as they are much smaller than the brighter, non-spherically shaped $BaCO_3$ particles [17]. Fig. 2A shows Pt clusters on Al_2O_3 corroborated by the corresponding EDX analysis detecting predominately Al and Pt and hardly any Ba (C and Cu peaks resulted form the TEM-grid). Similarly Fig. 2B illustrates the proximity of Pt on $BaCO_3$-particles with a strong Ba signal in the EDX spectra, also Al-peaks can be detected given the high Al-concentration in these $Pt/Ba/Al_2O_3$ catalysts (1:20:100). The presence of Pt did not influence measurably the characteristics of γ-Al_2O_3 or $BaCO_3$ as has been shown for TiO_2 [19]. All catalysts had a specific surface area (SSA) of about 140 m^2/g, while pure γ-Al_2O_3 had 148 m^2/g and pure $BaCO_3$ had 20 m^2/g, and

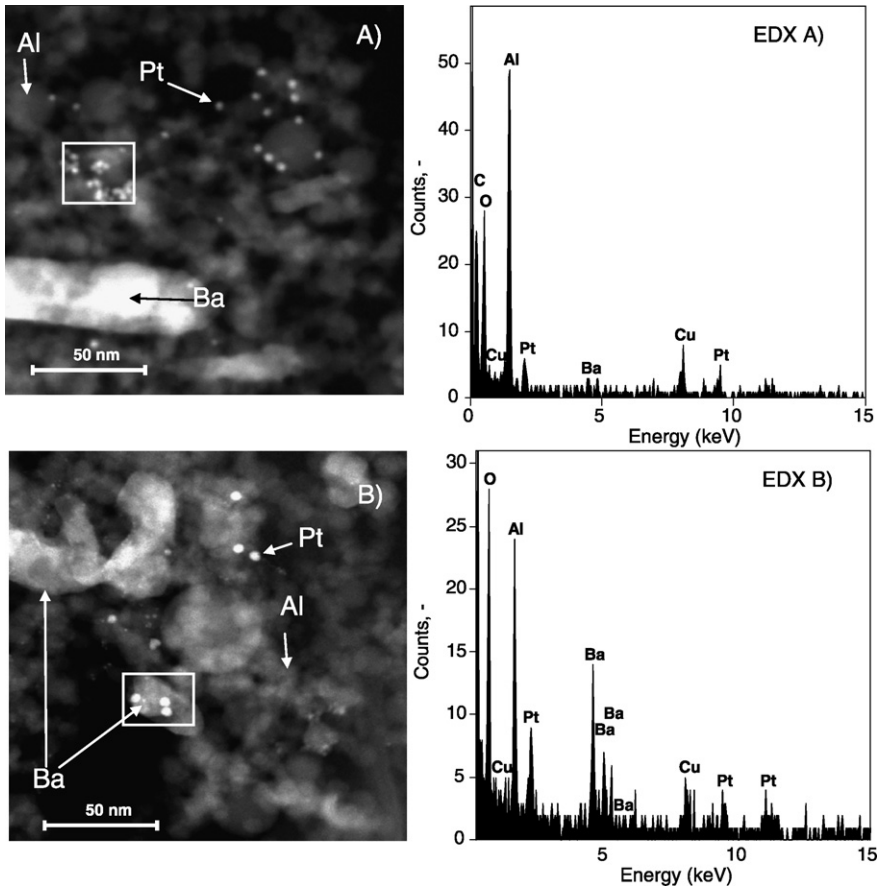

Fig. 2. Images of Pt preferentially deposited on Al_2O_3 (PtAl–Ba) (A) and $BaCO_3$ (Al–BaPt) (B). Corresponding EDX analysis of indicated areas are shown on the right.

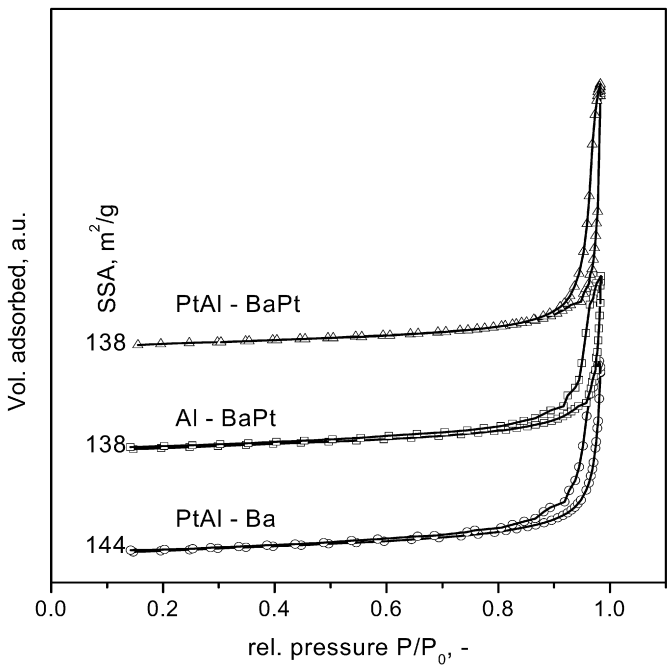

Fig. 3. Nitrogen adsorption–desorption isotherms of PtAl–BaPt, Al–BaPt, and PtAl–Ba along with the corresponding specific surface areas (SSA, m^2/g).

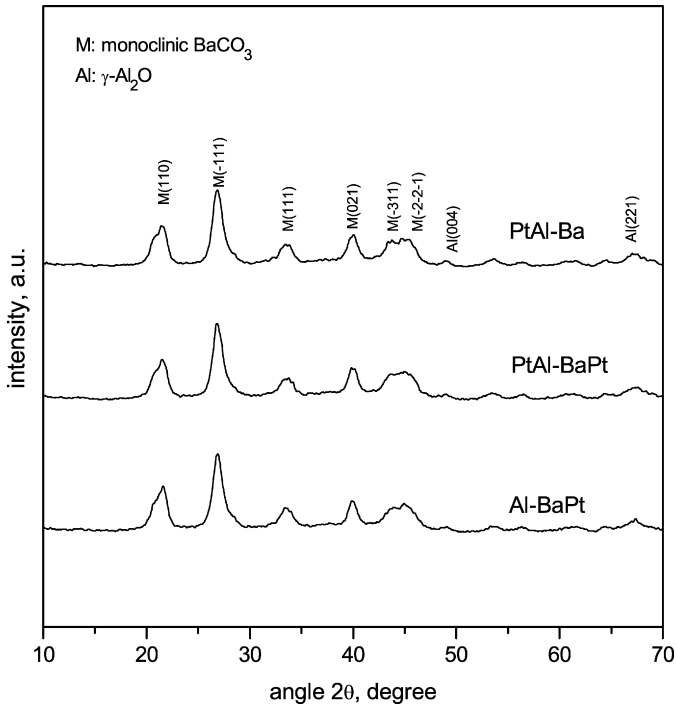

Fig. 4. XRD patterns of as-prepared catalysts. Characteristic reflections of monoclinic $BaCO_3$ (ICSD: 63257) and Al_2O_3 (ICSD: 99836) are indicated.

showed the typical isotherm of non-porous powders (Fig. 3) where the interparticle void gives rise to some hysteresis at high relative pressures. Fig. 4 shows the XRD patterns of the different catalysts indicating formation of monoclinic $BaCO_3$ in all samples. When stored at ambient conditions the monoclinic $BaCO_3$ gradually transforms into its more stable orthorhombic form [24].

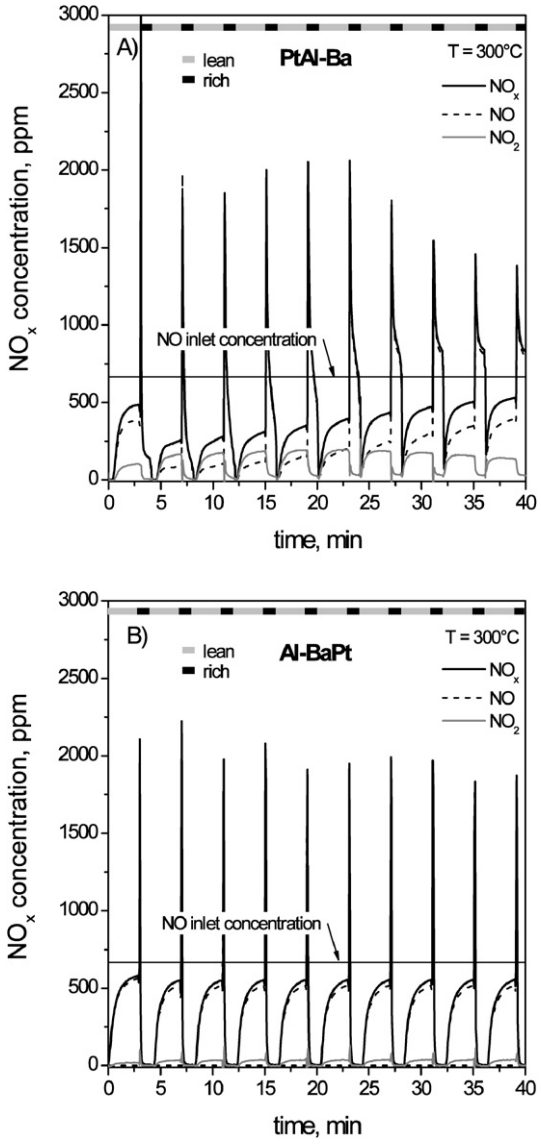

Fig. 5. Storage-reduction of NO with 667 ppm inlet concentration. Effluent gas concentrations (NO_x, NO, NO_2) during storage–reduction cycles at 300 °C for PtAl–Ba (A) and Al–BaPt (B).

The weight ratios of Al_2O_3:Ba:Pt were 100:20.1:1.1 for PtAl–Ba, 100:21.3:1 for Al–BaPt, and 100:20.5:1 for PtAl–BaPt measured by LA-ICP-MS matching well the nominal composition of Pt:Ba:Al_2O_3 = 1:20:100. The CO chemisorption on both PtAl–Ba and Al–BaPt materials indicated CO/Pt molar ratios of 0.30 and 0.25, respectively. The slightly lower Pt dispersion on the Ba component (Al–BaPt) corresponds well with Fig. 2, where the Pt size is similar and eventually slightly bigger for Al–BaPt. This may be attributable to the lower specific surface area of the support $BaCO_3$ compared to Al_2O_3 and the generally higher wetting angle of Pt on Al_2O_3. Larger specific surface areas prevent sintering of Pt clusters resulting in higher metal dispersions [25,26]. On $BaCO_3$ Pt tends to be oxidized to PtO_x [27] and the latter has a smaller wetting angle, an effect that can be used for redispersion of Pt [28].

3.2. Dynamic NO storage–reduction

First all results are shown at 300 °C where the different NSR behavior of the PtAl–Ba and Al–BaPt catalysts can be elucidated better. Fig. 5 shows the NO, NO_2 and NO_x outlet concentrations for a constant NO inlet flow under subsequent fuel lean (3 min) and rich (1 min) conditions for PtAl–Ba (A) and Al–BaPt (B). The difference between the NO inlet and NO_x outlet concentration is proportional to the NO_x stored on each catalyst. The Pt in the as-prepared catalysts is initially partially oxidized [29]. During the first-fuel rich cycle the Pt was activated, as seen in Fig. 5A, leading to better storage activity during the following cycles. During the first 5 cycles more NO is stored on PtAl–Ba but higher NO_2 concentrations are detected, indicating that the overall storage on PtAl–Ba is not limited by the NO oxidations but by the NO_2 uptake on Ba. This can be attributed to the high catalytic activity of Pt/Al_2O_3 to oxidize NO to NO_2, by a favorable metal–support interaction [7,27,30,31], in agreement with Cant et al. [11] who showed that Pt, when it is separated from the Ba component, solely serves to oxidize NO to NO_2 while slower NO_2 uptake on BaO was observed. For PtAl–Ba (Fig. 5A) the storage activity decreased continuously with time. As the barium nitrates were not completely regenerated during the fuel rich phases as the temperature for nitrate decomposition/reduction is too low, a close contact of Pt to Ba probably promotes the nitrate decomposition [15].

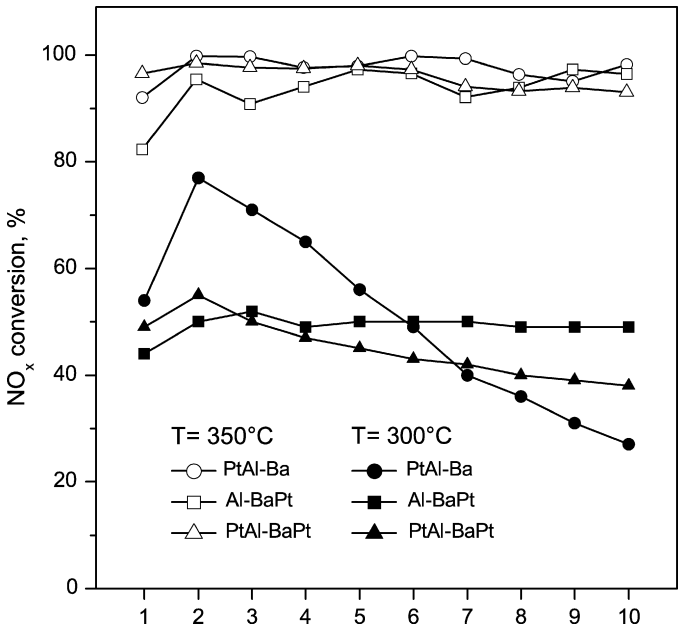

Fig. 6. NO_x conversion of the different NSR catalysts for each storage–reduction cycle at 300 (filled symbols) at 350 °C (open symbols).

For the Al–BaPt catalyst (Fig. 5B) the performance is constant during 10 cycles and highly reproducible (>130 cycles, not shown). Compared to PtAl–Ba, however, less NO is stored during the first cycles and a constant low effluent NO_2 was observed. After 3 min 87% of the inlet NO is already detected as NO_x in the effluent gas. Regeneration of this catalyst was significantly better than PtAl–Ba, especially at higher cycle numbers. This clearly shows the beneficial effect of having Pt close to Ba during regeneration. This close proximity has been attributed previously to Pt-promoted nitrate decomposition [15] and a higher reverse spillover [11]. Further, the close interaction of Pt and Ba not only facilitated $Ba(NO_3)_2$ decomposition, but also strongly increased the NO_x reduction activity. This may be attributed to the promotional effect of Ba on Pt during reduction [32].

Fig. 6 shows NO_x conversions for each fuel lean and a fuel rich period at 300 °C (filled symbols). The PtAl–Ba catalyst (circles) was most efficient for NO_x removal during the first cycles but lost progressively its efficiency from cycles 2 to 10 by its insufficient regeneration. After the 6th cycle the Al–BaPt catalysts performed better at a constant NO_x conversion. The catalysts with no prefer-

ential Pt deposition (PtAl–BaPt) perform in between the other two catalysts.

In Fig. 6 the catalysts were tested also at 350 °C (open symbols). For all catalysts more than 95% of NO inlet was reduced to N_2. Compared to 300 °C, all catalysts' performance was significantly better with good reduction and less deactivation at 350 °C. All showed similar performance due to fast NO to NO_2 oxidation on Pt regardless of support. As NO_x diffusion and adsorption were fast, the travel distance of Pt or Ba-species did not delay the overall process. At this temperature (350 °C), the thermodynamic stability of nitrates decreases [33], facilitating catalyst regeneration. This is expected as the optimal operation temperatures for $Pt/Ba/Al_2O_3$ catalysts are 350–400 °C [4]. An additional advantage could be the cycling between fuel lean and fuel rich phases, as the catalyst is often regenerated. This allowed surface reaction to be the major contribution in the NSR [34], avoiding the formation of bulk $Ba(NO_3)_2$ which changes the density (volume) and consequently the morphology of the particles. XRD analysis of selected samples showed no difference after dynamic NSR testing, indicating no bulk structural changes. Only after full NO_x saturation of the catalysts, Ba-nitrates could be detected (not shown).

3.3. Dynamic storage of NO_2

Experiments with NO_2 have been done to overcome the oxidation of NO to NO_2 that limited NO storage. This way, the role of Pt during actual storage of NO_2 could be understood better. Fig. 7A shows the storage–reduction of PtAl–Ba when NO_2 is fed. Again, the first cycle was needed to activate the Pt sites on the as-prepared catalysts. This catalyst could not store all incoming NO_2 as the off gas contained NO_2. As the regeneration of the catalysts during reduction was not sufficient, the activity continuously decreased as can be seen by the increasing NO_x in the exhaust. In contrast, almost all NO_2 is stored for Al–BaPt (Fig. 7B), compared to PtAl–Ba catalysts (Fig. 7A). This demonstrates the beneficial role of Pt being close to Ba during the actual storage [35] (in addition to Pt's role in oxidation of NO into NO_2). An effluent NO concentration of 270 ppm (as the NO_2 concentration is low $NO_x \approx NO$) was detected which corresponds to about 1/3 of the inlet NO_2. This agrees with Cant and Patterson [6], who postulated an overall storage reaction, whereby 3 NO_2 are needed for $Ba(NO_3)_2$ formation and one NO is released:

$$3NO_2 + BaCO_3 \rightarrow Ba(NO_3)_2 + NO + CO_2. \quad (2)$$

Compared to NO in the feed (Fig. 5), the absence of the necessary NO oxidation step resulted in a better NO_x uptake by Al–BaPt. Nevertheless, reduction seemed to be more difficult than with NO and the catalysts lost their storage capacity continuously. In this experiment the NO_2 inlet was kept constant also during reduction so $Ba(NO_3)_2$ decomposition takes place while NO_2 is reduced. Compared to feeding with NO, the catalysts fed with NO_2 showed insufficient regeneration, as fast NO_2 dissociation on Pt led to a higher oxygen partial pressure on the Pt [36]. The observed NO_2 to NO conversion does not need Pt, as Al_2O_3 alone can convert NO_2 to NO at 300 °C during fuel rich phases [37]. Full reduction of NO_2 needs therefore more time or higher temperatures to reduce the adsorbed NO_x species.

In Fig. 8 the overall NO_x conversion for different Pt location are compared. Similar to NO in the feed (Fig. 6), the performance of the PtAl–BaPt catalyst lies in between both catalysts. The NO_x conversions decreased for all three catalysts as the catalyst were not sufficiently regenerated at 300 °C.

3.4. Complete NO/NO_2 storage

The effect of storage time is elucidated in Fig. 9A which shows storage of NO at 300 °C, until the catalyst is saturated and the

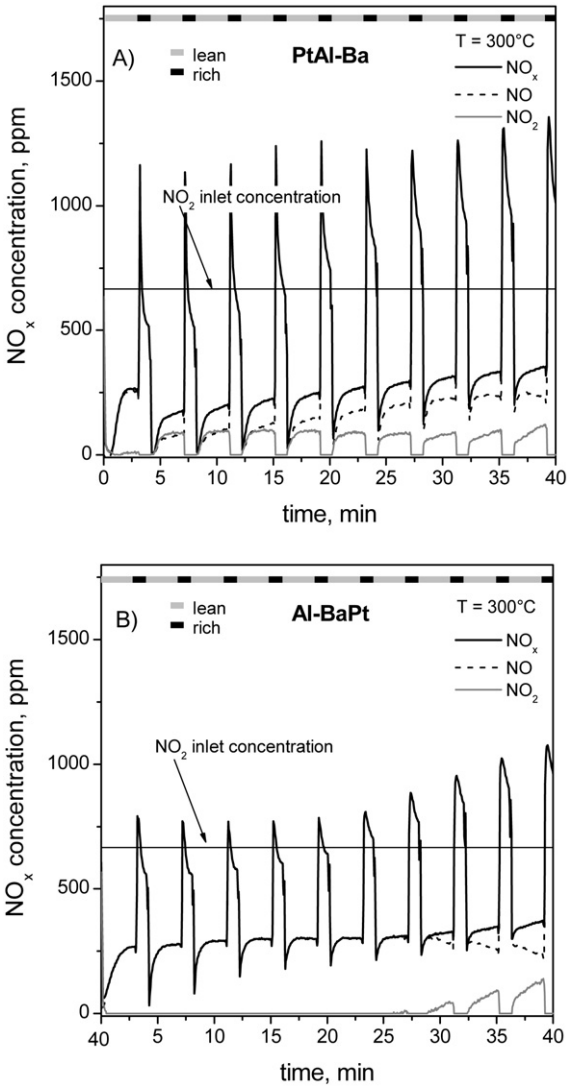

Fig. 7. Storage–reduction of NO_2. Effluent gas concentrations (NO_x, NO, NO_2) during storage–reduction cycles at 300 °C for PtAl–Ba (A) and Al–BaPt (B). NO_2 inlet concentration 667 ppm.

effluent NO_x reaches the NO inlet concentration. Note that here the catalysts were first reduced in C_3H_6 and therefore the NO_x uptake rate is almost twice that observed for untreated catalysts during the first 3 min. For Al–BaPt the initial NO_x emission was higher than for PtAl–Ba, however, both catalysts reached full saturation after about the same time and stored almost the same amount of NO, 1.22 and 1.25 $mmol_{NO}/g_{cat}$, respectively. This corresponds to a NO_x/Ba mol ratio of 1.1, which is only about 50% of the maximal theoretical uptake assuming complete conversion of $BaCO_3$ into $Ba(NO_3)_2$. The NO outlet concentration continuously increased and finally stabilized at 620 ppm. The concentration of NO_2 increased during the first 7 min to a maximum concentration of 120 ppm. This NO_2 maximum appeared later for Al–BaPt than for PtAl–Ba while NO_x increased slower, a sign that the initial overall NO_x storage is faster. After the maximum, the NO_2 concentration decreased and finally stabilized at around 50 ppm for both catalysts. This reduction of NO_2 might arise from the deactivation of Pt [27] caused by strong restructuring of the catalyst during $Ba(NO_3)_2$ formation resulting in Pt covered by Ba-nitrate [38]. This restructuring affects even the PtAl–Ba catalysts as their Al_2O_3 and $BaCO_3$ components are well-mixed and in close proximity to each other. Both catalysts reached nearly a steady state

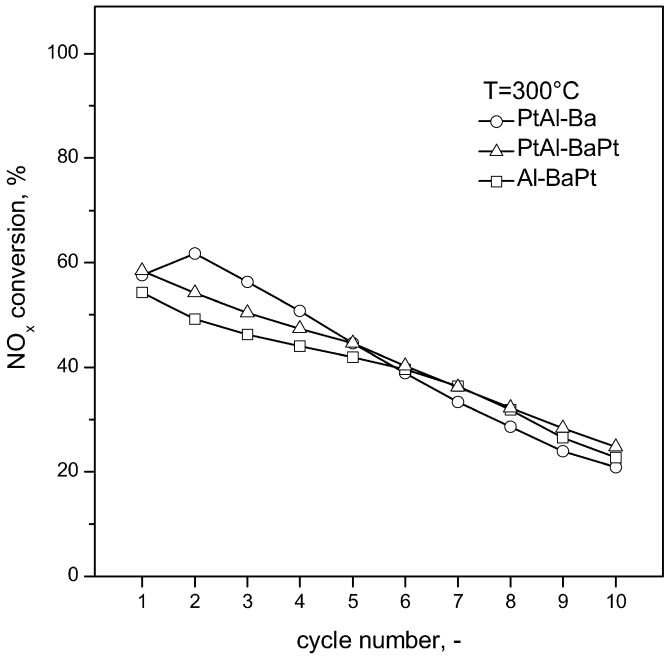

Fig. 8. NO_x conversion of the different NSR catalysts for each storage–reduction cycle for NO_2 in the feed at 300 °C.

where 7% NO is converted into NO_2, a 4-times lower conversion than on a Ba-free Pt-SiO_2 catalyst [39]. The similar NO/NO_2 outlet ratios for both catalysts suggest that the restructuring during full storage leads to a loss of the initial preferential positions of Pt, resulting in catalysts with similar structure and consequently similar catalytic activity. Compared to mechanically-mixed systems [11], the preferential Pt deposition applied here forms six times less NO_2 in the effluent gas. It seems that the gas-phase mixing in the flame process results in a more intimate contact between the various components.

Fig. 9B shows storage experiments with NO_2 as inlet gas. At the beginning of the storage only NO and no NO_2 was detected in the outlet gas, demonstrating that all inlet NO_2 is stored. After about 20 min the NO gas concentration increased to a maximum concentration of about $\frac{1}{3}$ of the NO_2 inlet concentration as predicted by Eq. (2) where $3NO_2$ are stored forming $Ba(NO_3)_2$, and releasing one NO. For the PtAl–Ba catalyst the NO maximum was reached faster (after 17 min) and still some effluent NO_2 was detected in the outlet gas, whereas Al–BaPt stored all NO_2 during the first 26 min illustrating again the beneficial effect of Pt close to Ba during NO_x uptake. Although some NO_2 slip was detected, the catalyst continued storing nitrous species until the NO_x concentration reached its inlet value and complete storage of 2.1 $mmol_{NOx}/g_{cat}$ of NO_2 was observed for both catalysts. This corresponds to a NO_x storage capacity of nearly 100% of the theoretical value.

The inlet gas composition, NO or NO_2, influences the storage behavior of $Pt/Ba/Al_2O_3$ catalysts, as seen when comparing Figs. 9A and 9B. Storage of NO is slow at 300 °C and only 50% of its maximum was stored whereas for NO_2 complete and faster storage was observed, whereby, during the storage, NO was formed and released. The differences in storage capacity for NO or NO_2 demonstrate the importance of active Pt for NO oxidation. During full storage this activity is lost due to restructuring and probably embedding of Pt in the resulting nitrates. As for NO_2 this oxidation step is not necessary. No active Pt is needed for NO_2 storage as complete conversion of $BaCO_3$ into $Ba(NO_3)_2$ takes place. At 300 °C the storage capacity is not limited by the storage compound but rather by the deactivation of Pt, as seen during NO storage. Longer storage times, however, are desirable for car catalysts, as less catalyst material would be needed for a given NO_x limit.

The limiting step for NSR catalysts is the regeneration especially at low temperatures and in the presence of sulfur and compounds that may poison the catalysts [4]. The good contact of Pt to the Ba could be the reason for the better regeneration of Al–BaPt catalysts where the spillover distance is smaller and Pt can interact with its support. The near contact of Pt to $BaCO_3$ may also cause some problems especially when considering aging where $BaCO_3$ and Pt can form $PtBaCO_3$ under lean conditions. However, catalysts containing the latter phase have been shown to be regenerable by reduction with hydrogen at relatively low temperature [40].

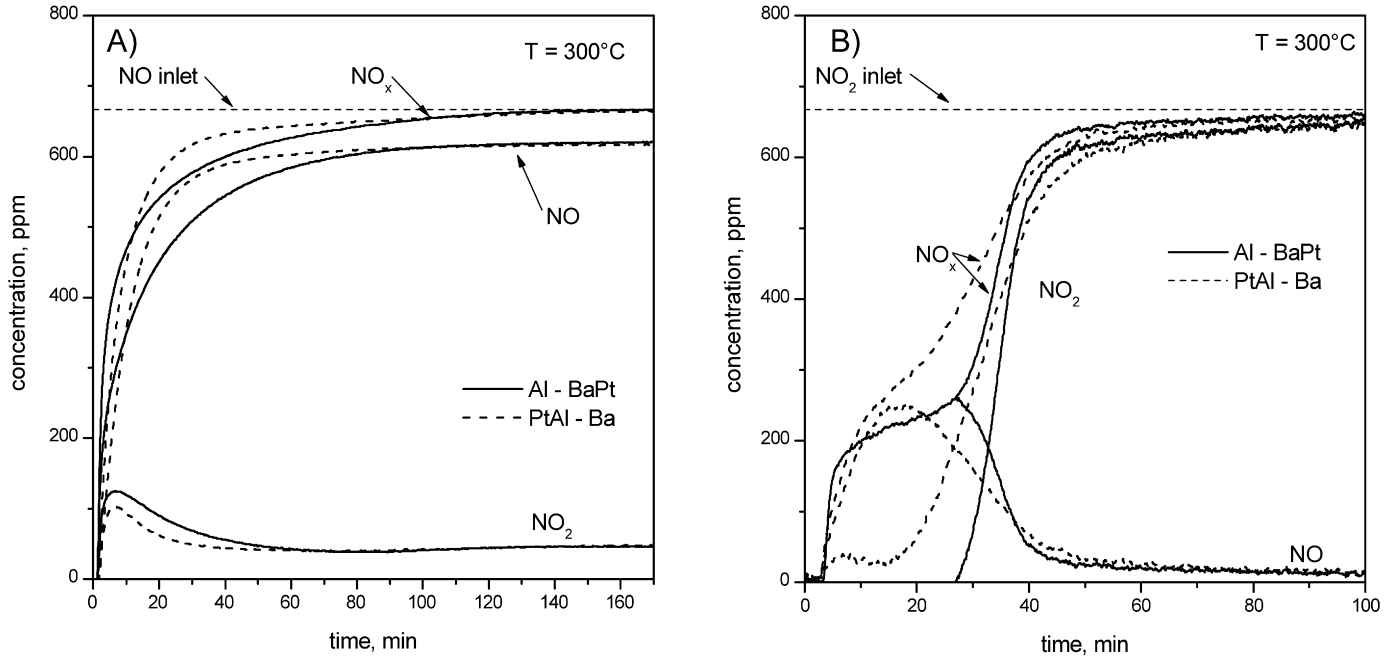

Fig. 9. Measured NO, NO_2 and NO_x outlet concentrations when Pt clusters are located predominantly on either Al_2O_3 (PtAl–Ba) or $BaCO_3$ (Al–BaPt), 3.3% O_2/He at 300 °C for 180 min with the inlet A) NO or B) NO_2 concentration of 666 ppm.

4. Conclusions

With a two nozzle flame spray pyrolysis unit $Pt/Ba/Al_2O_3$ catalysts with controlled deposition of Pt clusters on $BaCO_3$ or Al_2O_3 were prepared for studying the significance of Pt proximity to either Ba or Al in NO_x storage–reduction catalysts.

During storage, the beneficial role of a close interaction of Pt and Ba for NO_x uptake could be confirmed. However, Pt on Al_2O_3 exhibited a better NO oxidation activity which was the limiting step for the overall NO storage process at low temperatures (300 °C). During reduction, Pt on Ba showed much better activity than Pt on Al_2O_3. This can be attributed to the importance of reverse spill-over and the promotional effect of Ba on the Pt reduction activity. Storage of NO and NO_2 until saturation revealed that the storage capacity is not limited by Ba but by the loss of Pt oxidation activity during catalyst restructuring. At higher temperatures (350 °C), the location of Pt barely affected the performance during storage and reduction. Therefore spill over is not a limiting step anymore. These differences of activity of Pt in contact with Al or Ba can be exploited for the design of NSR catalysts with improved performance at low temperatures.

Acknowledgments

We thank Prof. Detlef Günther (ETH) and Kathrin Hametner (ETH) for the LA-ICP-MS measurements. We kindly acknowledge financial support by ETH Zurich (TH-09 06-2) and thank the Electron Microscopy Center of ETH Zurich (EMEZ) for providing the necessary infrastructure. The contribution of platinum chemicals by Johnson Matthey PLC is greatly appreciated.

References

[1] J. Zeldovich, Acta Physicochim. URSS 21 (1946) 577.
[2] R. Atkinson, A.C. Lloyd, J. Phys. Chem. Ref. Data 13 (1984) 315.
[3] N. Takahashi, H. Shinjoh, T. Iijima, T. Suzuki, K. Yamazaki, K. Yokota, H. Suzuki, N. Miyoshi, S. Matsumoto, T. Tanizawa, T. Tanaka, S. Tateishi, K. Kasahara, Catal. Today 27 (1996) 63.
[4] W.S. Epling, L.E. Campbell, A. Yezerets, N.W. Currier, J.E. Parks, Catal. Rev. Sci. Eng. 46 (2004) 163.
[5] A. Casapu, J.D. Grunwaldt, M. Maciejewski, F. Krumeich, A. Baiker, M. Wittrock, S. Eckhoff, Appl. Catal. B 78 (2008) 288.
[6] N.W. Cant, M.J. Patterson, Catal. Today 73 (2002) 271.
[7] B. Subramaniam, A. Varma, Chem. Eng. Commun. 20 (1983) 81.
[8] L. Olsson, H. Persson, E. Fridell, M. Skoglundh, B. Andersson, J. Phys. Chem. B 105 (2001) 6895.
[9] Z.Q. Liu, J.A. Anderson, J. Catal. 224 (2004) 18.
[10] N. Miyoshi, S. Matsumoto, K. Katoh, T. Tanaka, J. Harada, N. Takahashi, K. Yokota, M. Sugiura, K. Kasahara, SAE Technical Paper 950809, 1995.
[11] N.W. Cant, I.O.Y. Liu, M.J. Patterson, J. Catal. 243 (2006) 309.
[12] K.S. Kabin, R.L. Muncrief, M.P. Harold, Catal. Today 96 (2004) 79.
[13] S. Balcon, C. Potvin, L. Salin, J.F. Tempere, G. Djega-Mariadassou, Catal. Lett. 60 (1999) 39.
[14] A. Amberntsson, H. Persson, P. Engstrom, B. Kasemo, Appl. Catal. B 31 (2001) 27.
[15] I. Nova, L. Lietti, L. Castoldi, E. Tronconi, P. Forzatti, J. Catal. 239 (2006) 244.
[16] I. Nova, L. Castoldi, L. Lietti, E. Tronconi, P. Forzatti, SAE Technical Papers 2006-01-1368, 2006.
[17] R. Strobel, L. Madler, M. Piacentini, M. Maciejewski, A. Baiker, S.E. Pratsinis, Chem. Mater. 18 (2006) 2532.
[18] M. Piacentini, R. Strobel, M. Maciejewski, S.E. Pratsinis, A. Baiker, J. Catal. 243 (2006) 43.
[19] H. Schulz, L. Madler, R. Strobel, R. Jossen, S.E. Pratsinis, T. Johannessen, J. Mater. Res. 20 (2005) 2568.
[20] L. Madler, W.J. Stark, S.E. Pratsinis, J. Mater. Res. 17 (2002) 1356.
[21] D. Gunther, C.A. Heinrich, J. Anal. At. Spectrom. 14 (1999) 1363.
[22] R. Strobel, F. Krumeich, S.E. Pratsinis, A. Baiker, J. Catal. 243 (2006) 229.
[23] J.A. Phil, J.E.P. Il, C.S. Daw, T.W. Root, SAE 2006-01-3441, 2006.
[24] R. Strobel, M. Maciejewski, S.E. Pratsinis, A. Baiker, Thermochim. Acta 445 (2006) 23.
[25] R. Strobel, F. Krumeich, W.J. Stark, S.E. Pratsinis, A. Baiker, J. Catal. 222 (2004) 307.
[26] A.N. Kholodovich, P.A. Simonov, React. Kinet. Catal. Lett. 86 (2005) 381.
[27] L. Olsson, E. Fridell, J. Catal. 210 (2002) 340.
[28] E. Ruckenstein, Y.F. Chu, J. Catal. 59 (1979) 109.
[29] S. Hannemann, J.D. Grunwaldt, P. Lienemann, D. Gunther, F. Krumeich, S.E. Pratsinis, A. Baiker, Appl. Catal. A 316 (2007) 226.
[30] F. Prinetto, G. Ghiotti, I. Nova, L. Lietti, E. Tronconi, P. Forzatti, J. Phys. Chem. B 105 (2001) 12732.
[31] M. Sasaki, H. Hamada, Y. Kintaichi, T. Ito, Catal. Lett. 15 (1992) 297.
[32] M. Konsolakis, I.V. Yentekakis, J. Catal. 198 (2001) 142.
[33] Y.J. Li, S. Roth, J. Dettling, T. Beutel, Top. Catal. 16 (2001) 139.
[34] E. Fridell, H. Persson, L. Olsson, B. Westerberg, A. Amberntsson, M. Skoglundh, Top. Catal. 16 (2001) 133.
[35] P. Forzatti, L. Castoldi, I. Nova, L. Lietti, E. Tronconi, Catal. Today 117 (2006) 316.
[36] A.J. Desai, E.A. Lombardo, V.I. Kovalchuk, J.L. d'Itri, Catal. Lett. 72 (2001) 65.
[37] G.R. Bamwenda, A. Obuchi, A. Ogata, J. Oi, S. Kushiyama, K. Mizuno, React. Kinet. Catal. Lett. 63 (1998) 53.
[38] J. Szanyi, J.H. Kwak, J. Hanson, C.M. Wang, T. Szailer, C.H.F. Peden, J. Phys. Chem. B 109 (2005) 7339.
[39] J.M.G. Cortes, M.J.I. Gomez, C.S.M. de Lecea, Appl. Catal. B 74 (2007) 313.
[40] M. Casapu, J.D. Grunwaldt, M. Maciejewski, A. Baiker, R. Hoyer, M. Wittrock, S. Eckhoff, Catal. Lett. 120 (2008) 1.